New isomeric transition in ^{36}Mg: Bridging the $N = 20$ and $N = 28$ islands of inversion

M. Madurga,[1] J. M. Christie,[1] Z. Xu,[1] R. Grzywacz,[1,2] A. Poves,[3] T. King,[1] J. M. Allmond,[2] A. Chester,[4]
I. Cox,[1] J. Farr,[1] I. Fletcher,[1] J. Heideman,[1] D. Hoskins,[1] A. Laminack,[2] S. Liddick,[4,5] S. Neupane,[1] A. L. Richard,[4,*]
N. Shimizu,[6] P. Shuai,[1,2,†] K. Siegl,[1] Y. Utsuno,[7,8] P. Wagenknecht,[1] and R. Yokoyama[1]

[1]*Deptartment of Physics and Astronomy, University of Tennessee, Knoxville, Tennessee 37996, USA*
[2]*Physics Division, Oak Ridge National Laboratory, Oak Ridge, Tennessee 37830, USA*
[3]*Departamento de Física Teórica, and IFT UAM-CSIC, Universidad Autónoma de Madrid, 28049 Madrid, Spain*
[4]*National Superconducting Cyclotron Laboratory, Michigan State University, East Lansing, Michigan 48824, USA*
[5]*Department of Chemistry, Michigan State University, East Lansing, Michigan 48824, USA*
[6]*Center for Computational Sciences, University of Tsukuba, 1-1-1, Tennodai Tsukuba, Ibaraki 305-8577, Japan*
[7]*Advanced Science Research Center, Japan Atomic Energy Agency, Tokai, Ibaraki 319-1195, Japan*
[8]*Center for Nuclear Study, University of Tokyo, Hongo, Bunkyo-ku, Tokyo 113-0033, Japan*

We observed a new isomeric γ transition at 168 keV in ^{36}Mg, with a half-life of $T_{1/2} = 90(^{+410}_{-50})$ ns. We propose that the observed transition deexcites a new 0^+ isomeric state at 833 keV and populates the previously known first 2^+ state. The existence of this isomer is consistent with the predictions of the large-scale shell-model calculations of ^{36}Mg using the *sdpf-u-mix* interaction. The observed excitation energy of the second 0^+ state is caused by the small energy separation between two prolate-deformed configurations where the intruder configuration corresponds to two-neutron excitations from the sd to the pf shell. Within this interpretation, ^{36}Mg becomes the crossing point between nuclei in which ground state deformed/superdeformed configurations are caused by the dominance of $N = 20$ intruders (^{32,34}Mg) and nuclei where deformed configurations are associated with the breaking of the $N = 28$ closure and a large occupancy of the $1p_{3/2}$ neutron orbit (^{38}Mg and beyond). We found the lack of three-body monopole corrections in other effective interactions results in a predominance of $N = 20$ intruder configurations past ^{38}Mg incompatible with our observation. We conclude that ^{36}Mg bridges the $N = 20$ and $N = 28$ islands of inversion, forming the so-called big island of deformation.

Introduction. The large shell gaps in nuclei with "magic" numbers for protons and neutrons emerge from the collective action of the strong forces mediated through pion exchange. However, most nuclei are nonmagic, and many are deformed due to the effects of nucleon-nucleon correlations. The surprising emergence of the so-called islands of inversion, where the nuclei with magic numbers are known to be deformed, was attributed to the dominating character of correlations due to the quenching of the shell gaps.

The island of inversion centered around magnesium isotopes with the neutron magic number $N = 20$ has attracted considerable interest [1–5] since its discovery [6]. Negative-parity intruder states ascribed to excitations involving multiple particle-hole configurations between sd and pf orbitals indicate a sudden quenching of the $N = 20$ shell closure. Nuclei inside the island of inversion are defined by having ground states dominated by such configurations [7]. Further, recent experimental [8] and theoretical [5] studies suggest that particle-hole configurations dominate ground states in this region of the chart of nuclei between the $N = 20$ and the $N = 28$ magic numbers. This forms a so-called big island of deformation, where both neutron magic numbers $N = 20$ and $N = 28$ disappear in the magnesium isotopic chain. The quenching of the $N = 20$ and $N = 28$ neutron gaps is driven by the diminishing effect of the isospin $T = 0$ component of the tensor force as the proton-neutron ratio becomes more asymmetric [9]. Recently developed interactions in the proton and neutron sd-pf valence space have had considerable success in reproducing the observed intruder and ground-state configurations of known island of inversion nuclei. Some examples are effective interactions such as *sdpf-m* [10], which only includes the $0f_{7/2}$ and $1p_{3/2}$ neutron orbits, and we disregard *sdpf-u-mix* [5] or the new interaction *EEdf1*, developed from the chiral expansion at N3LO. [11] As we see later, the explicit three-body global monopole term proposed with *sdpf-u-mix* is crucial to produce the evolution of the $N = 20$ neutron closure towards $N = 28$ consistent with our observation. Interestingly, both interactions predict differing microscopic interpretations of the merging of the $N = 20$ and $N = 28$ islands of inversion. In *EEdf1*, excited states crossing

*Current address: Institute of Nuclear and Particle Physics and Department of Physics and Astronomy, Ohio University, Athens, Ohio 45701, USA.

†Current address: Institute of Modern Physics, Chinese Academy of Sciences, Lanzhou, Gansu 730000, China.

the $N = 20$ shell closure are substantial in both islands of inversion. On the other hand, *sdpf-u-mix* predicts the restoration of the $N = 20$ shell closure at ^{40}Mg, postulating instead that deformation is driven exclusively by the breakdown of the $N = 28$ subshell closure. There are currently no experimental data that can resolve these differing interpretations. Delineation of the boundaries of the islands of inversion towards the neutron drip-line is therefore essential to determine the disappearance and appearance of the $N = 20$ and $N = 28$ shell closures, respectively [12]. Isomers, long-lived excited states, offer an observable with which to track evolving nuclear properties as we study nuclei between shell closures. The half-life of an isomeric state is fully determined by the transition's energy and its electromagnetic transition probability, in turn, is defined by the wave functions of the involved states. One such example are the so-called shape isomers, excited states arising from nuclear configurations of different shapes. Low-energy excited 0^+ states corresponding to prolate-deformed (oblate-deformed) configurations [13] may become isomeric when decaying to the first excited 2^+ state corresponding to the ground state band of a different deformation.

As of the beginning of 2023, there has been only one isomer confirmed and published in either neon or magnesium isotopes, the 0_2^+ state in ^{32}Mg that decays to the 2_1^+ state via a 172-keV transition with $T_{1/2} > 10$ ns [14,15]. Shell-model calculations using the *sdpf-u-mix* interaction [16] produce a ground state that is a mixture of deformed ($2\hbar\omega$) and superdeformed ($4\hbar\omega$) configurations and an isomeric 0^+ state that is dominated by superdeformed and spherical ($0\hbar\omega$) components [5]. Notice that *sdpf-u-mix* is the only interaction that locates the isomer close to its experimental excitation energy. In the same calculation, heavier magnesium isotopes were expected to strongly favor quadrupole components before transitioning to the $N = 28$ island of inversion at ^{40}Mg. This hypothesis is supported by the systematics of the first 2^+ states in ^{34,36,38}Mg [8,17–19], comparing well with calculations [20].

In this work we present the observation of a new isomeric γ transition at 168 keV in ^{36}Mg. Based on the observation of a 665-keV γ line, likely corresponding to the 2^+ state in ^{36}Mg, we propose it corresponds to a second 0^+ state feeding said first 2^+ state. The analysis of the time structure of 168-keV γ-ray events following the ion implantation results in a half-life of $T_{1/2} = 90(^{+410}_{-50})_{\text{stat}}(\pm 40)_{\text{tran}}(^{+800}_{-70})_{\text{sys}}$ ns ("tran" corresponds to the uncertainty due to the transit time A1900, see below). We present an interpretation of the nature of the new second 0^+ state and the evolution of intruder configurations in the magnesium isotopic chain from $N = 20$ to $N = 28$ using shell-model with configuration interaction (SM-CI) calculations with the *sdpf-u-mix* interaction [5]. Our calculations indicate the isomer naturally arises from gradually restoring the $N = 20$ shell closure as the neutron $0f_{7/2}$ orbital is occupied towards the $N = 28$ subshell closure.

Experiment. The experiment was performed at the National Superconducting Cyclotron Laboratory (NSCL) at Michigan State University. A ^{48}Ca beam, with 80-pnA average intensity at 140 MeV/u, was fragmented in a 846-mg/cm^2-thick Be target at the entrance of the fragment separator, A1900 [21], to produce the nuclei of interest, a "cocktail" beam consisting
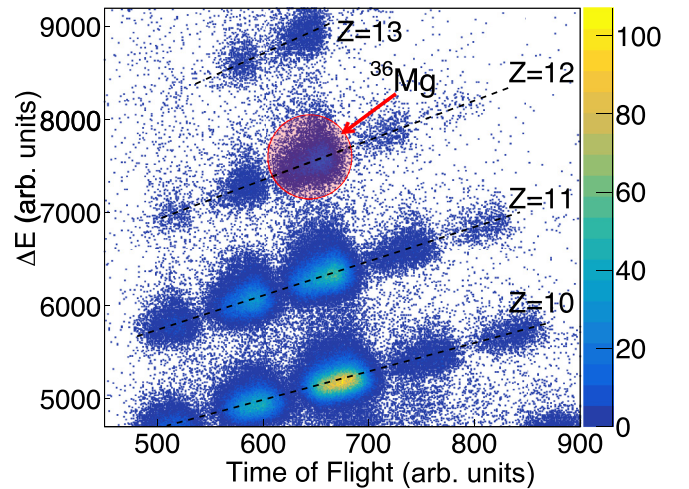

FIG. 1. Two-dimensional energy loss (ΔE) vs time-of-flight particle identification plot for all ion implants between $Z = 10$ (bottom row) and $Z = 13$ (top row). Magnesium-36 is highlighted by the red circle. We also searched for isomers in $^{25-29}$F isotopes (not shown).

of isotopes from boron ($Z = 5$) to aluminum ($Z = 13$). In order to identify the different species, we measured the ion's time-of-flight between a scintillator located in the focal plane of A1900 and a silicon detector (Si PIN) placed in front of our experimental setup. Combining with the energy loss in the Si PIN allowed us to perform particle identification (PID) in the beam, as shown in Fig. 1. We implanted the "cocktail" beam in a 12-mm-thick YSO detector (yttrium orthosilicate, Y_2SiO_5) [22] allowing for recording energies and time stamps of ion implantation and β-decay events. The YSO detector was surrounded on one side by 48 VANDLE modules [23], providing a total neutron detection efficiency of 11% at 1 MeV. On the other side of the setup, there were three high-purity germanium (HPGe) clovers from the CLAR-ION array [24] resulting in γ detection of 1.3% efficiency at 1 MeV.

We searched for isomers in all fluorine, neon, sodium, magnesium, and aluminum isotopes shown in Fig. 1 by analyzing the γ rays emitted between 40 and 500 ns after ion implantation, correlated to each individual isotope using the PID plot (Fig. 1). We excluded the first 40 ns in order to remove the Gaussian tail of the prompt implantation "flash." We did not identify isomeric transitions in any F, Ne, Na, Mg, or Al isotopes except for ^{36}Mg (^{32}Mg was outside of the separator acceptance in our experiment). In ^{36}Mg, we observe a prominent γ transition at 168 keV (see Fig. 2). The top right inset of Fig. 2 shows the γ spectrum between 500 and 750 keV. We marked several γ lines (†) corresponding to neutron inelastic scattering in common HPGe materials [25], as well as the 511-keV line corresponding to positron annihilation (#). We observe 4(2) counts (all errors in this section are statistical at 1σ confidence level) in the energy region where the 665-keV deexcitation of the first excited state in ^{36}Mg [8,17,18,26–28] would be located. The spin and parity of the first excited state of ^{36}Mg was confirmed to be 2^+ by the recent measurement of the quadrupole electromagnetic transition strength [18]. Since
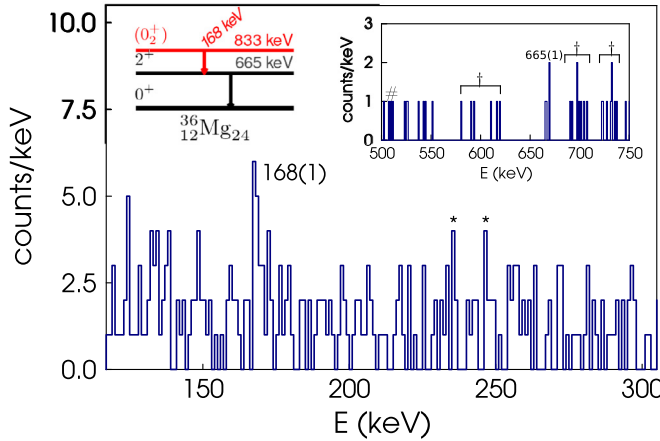
FIG. 2. Delayed γ energy spectrum in coincidence with ^{36}Mg implantation events. The most prominent line corresponds to the new isomeric transition at 168 keV ([*] marks background lines). The top left inset shows the ^{36}Mg partial level scheme. The top right inset shows the γ spectrum between 500 and 750 keV, including the ^{36}Mg 665-keV transition and other background lines (see text for details).
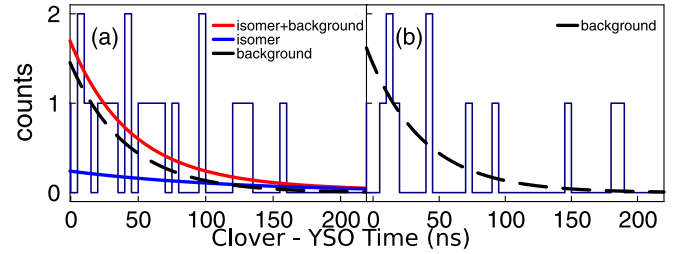

FIG. 3. (a) Time distribution of γ activity after ion implantation gated on the 168-keV photopeak with background [black-dashed, see panel (a)], isomer (blue), and combined (red) fits overlaid. (b) Distribution of γ events gated on the Compton background surrounding the photopeak.

the state was not observed to be isomeric, we propose the isomeric state in ^{36}Mg decays to the 2^+ state via emitting the 168-keV γ ray. We calculated the number of counts we would observe if the new 168-keV line and the 665-keV line formed a γ cascade. We observe 8(4) counts in the 168-keV peak above background. Using efficiencies of 1.8% at 168 keV and 1.5% at 665 keV we expect 6(3) counts at 665 keV, compatible with the observed 4(2) counts. Imposing total event multiplicity and using the complete data set with no isotope selection, we observe nothing but Compton background in the 640- to 680-keV region. To further validate our hypothesis, the presence of a 665-keV line, we performed a statistical study using the Monte Carlo method, obtaining a confidence level of 2.8σ. Assuming the two lines are in coincidence, as presented by the evidence above, we propose that the 168-keV isomer deexcites a new 833-keV state directly to the known 665-keV 2_1^+ state in ^{36}Mg (top left inset in Fig. 2). The spin-parity of this new state cannot be directly measured in this experiment. However, we can identify possible candidates and rule out impossible combinations. Given the strong evidence for the first 2^+ state to correspond to the first excited state of a prolate rotational band [18], any positive-parity member of the band would not be isomeric. We can also rule out negative-parity states of spin higher than 0 and lower than 4, as they would decay to the 2^+ state via an $E1$ transition, typically too fast to be isomeric. This leaves $0^{+,-}$, and 4^- and higher, as the best candidate spin-parities. Provided the state is at 833 keV, it would be below the pairing gap, therefore making it very unlikely to be a negative-parity state. We conclude 0^+ is the most likely spin-parity, corresponding well to the the other known isomer in neutron-rich magnesium isotopes (the second 0^+ state in ^{32}Mg [14]).

We performed a log likelihood analysis of the γ activity after ion implantation to determine the isomer's half-life (see Fig. 3). Figure 3(a) shows the time distribution of γ events after ion implantation for the photopeak gate (167 to 169 keV).

Figure 3(b) shows the time distribution of background events ($166 < E_\gamma < 167$ keV and $169 < E_\gamma < 170$ keV). First, in order to estimate the component arising from the tail of the Gaussian distribution of the ion implantation Bremsstrahlung flash, we fitted the time distribution of the background gate to an exponential function [Fig. 3(b)]. Then, we constructed a double-exponential distribution, corresponding to the photopeak and the background combined, 50% each as per the γ energy spectrum estimate. We fitted the photopeak gate, obtaining $T_{1/2} = 90(^{+410}_{-50})$ ns. We also studied the systematic uncertainty due to the shape of the tail of the implantation flash. In order to progressively remove the background tail, we performed fits to samples starting at increasingly later times, between 50 and 100 ns. Finally, we calculated the shortest observable half-life considering the transit time (500 ns) in A1900 and assuming an isomer population of 10% (or a larger population of 40%) in the fragmentation reaction producing ^{36}Mg, obtaining 130 ± 40 (90 ± 30 for 40% isomer population) ns. Given the statistical constraints due to the size of our sample (3σ statistical uncertainty in parentheses and marked as "stat"), the limits imposed by the transit time in A1900 (uncertainty in parentheses and marked with "tran"), and the systematic effects mentioned above (uncertainty in parentheses and marked with "sys"), we provide a half-life for the 168-keV isomer of $T_{1/2} = 90(^{+410}_{-50})_{\text{stat}}(\pm40)_{\text{tran}}(^{+800}_{-70})_{\text{sys}}$ ns. The resulting half-life corresponds to $B(E2) = 70(^{+80}_{-60})_{\text{stat}}(^{+30}_{-40})_{\text{tran}}(^{+210}_{-60})_{\text{sys}}\ e^2\ \text{fm}^4$.

Discussion. In the heavy magnesium isotopes, two neutron magic numbers are washed out by the presence of intruder configurations whose energy, fostered by the quadrupole correlations and the reductions of the spherical $N = 20$ and $N = 28$ gaps, makes them dominant in the ground states, giving rise to the $N = 20$ and $N = 28$ islands of inversion. As explained in Ref. [5] we submit that the effective interaction for this wide region should include a three-body monopole correction of the following form:

$$\delta V_{pf} = \frac{1}{2} n_{pf} \left(\frac{18}{A}\right)^{1/3} 75 \text{ keV}, \tag{1}$$

which restores the $N = 20$ closure in ^{40}Mg as it is required by consistency and naturalness of the very SM-CI approach (n_{pf} is the number of neutrons in the pf shell in the normal-filling approximation). Notice, however, that in Ref. [29] the *EEdf1*
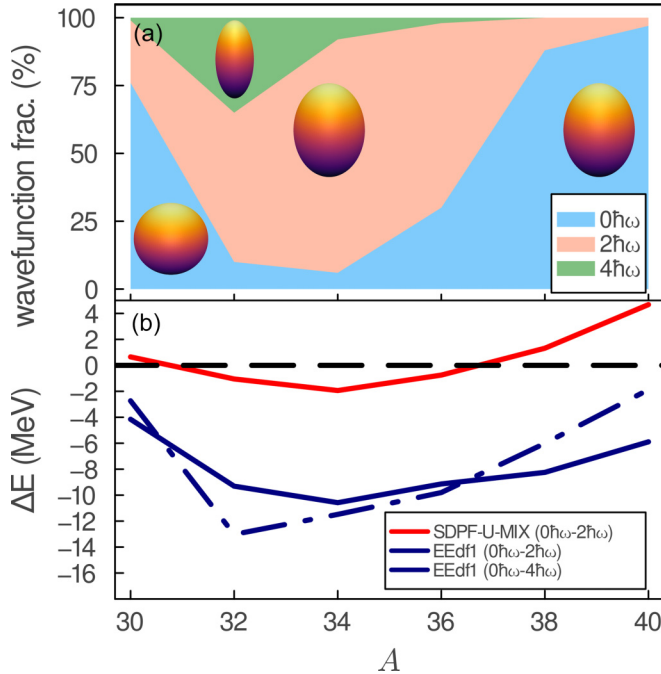
FIG. 4. (b) Energy splitting between the normal-filling configuration and the intruder state corresponding to the promotion of two neutrons across the $N = 20$ magic shell closure ($2\hbar\omega$), in the heavy magnesium isotopes, calculated with *sdpf-u-mix* (red line) and *EEdf1* (solid blue line corresponds to $2\hbar\omega$ and dash-dotted blue line corresponds to four neutron excitations $4\hbar\omega$). (a) Percentage of $x\hbar\omega$ configurations in the theoretical wave functions of the ground states of the magnesium isotopes, $0\hbar\omega$ (blue), $2\hbar\omega$ (orange), and $4\hbar\omega$ (green), using the *sdpf-u-mix* interaction. The cartoon nuclei represent the shape of each configuration.

interaction produces a completely different picture because the neutron $0d_{3/2}$ orbit is only half filled already in ^{30}Mg and remains so even in the ^{40}Mg ground state. With the interaction *sdpf-u-mix*, the $N = 20$ neutron gap in ^{40}Mg is 1 MeV smaller that in ^{32}Mg, and the amount of $2\hbar\omega$ components in the former is about 25%. Including the three-body correction, the effective $N = 20$ neutron gap in ^{40}Mg increases 2 MeV and the $2\hbar\omega$ components go down to less than 5%.

We proceed now to explain the results of our SM-CI calculations using the *sdpf-u-mix* interaction [5]. The calculations are performed with the code ANTOINE [30]. It is interesting to follow the location of the intruder configurations before mixing as the number of neutrons increase. We denote by $0\hbar\omega$ the normal-filling configuration, and by $x\hbar\omega$, with $x = 0, 2, 4$, etc., the xp-xh neutron excitations across $N = 20$. Their relative position gives us a clear hint of what will be the structure of the low-lying states after full diagonalization, although the details of the spectroscopy depend on many other ingredients, in particular, on the off-diagonal matrix elements between the states calculated at fixed values of $x\hbar\omega$ differing in two units. As a first step, we study the relative location of the 0^+ band heads of the $0\hbar\omega$ and $2\hbar\omega$ configurations. The results are shown in Fig. 4(b). It is seen that the intruder states cease to be clearly dominant at $A = 36$. The increase of the quadrupole moment Q_{spec} of the $2\hbar\omega$ configuration with respect to the

$0\hbar\omega$ one is small; therefore, the gain in quadrupole correlation energy of the latter barely compensates its loss of monopole energy. As a consequence, the $2\hbar\omega$ configuration in ^{36}Mg is not as dominant as the one in ^{34}Mg. Beyond $A = 36$ ($N = 24$), the $0\hbar\omega$ configurations are re-established as the main components in the ground states of ^{38}Mg and ^{40}Mg. This is in stark contrast with the calculation using the *EEdf1* interaction shown in Fig. 4(a). Here, intruder configurations, both $2\hbar\omega$ and $4\hbar\omega$, remain dominant across the entire isotopic chain, precluding mixing with $0\hbar\omega$ normal-filling configurations. However, we must point out, as seen in Fig. 4, that the energies of the $2\hbar\omega$ and $4\hbar\omega$ configurations are quasidegenerate for ^{34}Mg and ^{36}Mg. As we see later, large off-diagonal elements in *EEdf1* result in a strong repulsion when considering two-state mixing, resulting in high-energy 0_2^+ states except for the postulated second 0^+ state in ^{40}Mg [29].

It is precisely the crossing of the $0\hbar\omega$ and $2\hbar\omega$ configurations in ^{36}Mg that might explain the very low energy of the proposed 0_2^+ state. In the full calculation, *sdpf-u-mix* places the excited 0^+ in ^{36}Mg at 1.55 MeV and produces a ^{36}Mg isotope that is not axially symmetric (triaxial) with low-energy excitations (γ band). These low-energy states are not compatible with the existence of a 0^+ isomer as proposed in the present experiment. Given that the amplitude of the $4\hbar\omega$ configurations is negligible, the problem can be translated into a two-state model including only the $0\hbar\omega$ and $2\hbar\omega$ states discussed above. According to the calculated Q_{spec} moments within the bands, both are prolate deformed. If the energies of the $0\hbar\omega$ and $2\hbar\omega$ states were degenerate before mixing (and this is nearly the case), the final splitting of the two 0^+ states would be roughly equal to $2W$, with $W = \langle 0\hbar\omega(0^+)|V|2\hbar\omega(0^+)\rangle$. In fact, $W = 730$ keV in ^{36}Mg, and this sets a theoretical lower limit to the excitation energy of the isomer 0^+, within the two-state model. The value in the complete diagonalization is very much in line with this estimate. Thus, the only way to get the splitting right is via a reduction of the value of W, which is dominated by the off-diagonal pairing interaction between the sd- and the pf-shell neutron orbits. Hence we are led to make an "ad hoc" 10% reduction of the off-diagonal pairing matrix elements for $n_{pf} > 0$, bringing W down to about 500 keV. With this choice, the resulting composition of the ground states of the magnesium isotopes is as depicted in Fig. 4(a). We see that the intruder ($2\hbar\omega$, $4\hbar\omega$) configurations are dominant in ^{32,34,36}Mg, while the normal-filling ($0\hbar\omega$) states take the majority of the wave function in ^{30,38,40}Mg. This trend is consistent with the restoration of the $N = 20$ shell closure as we approach the $N = 28$ sub-shell, disfavoring particle-hole excitations across the $N = 20$ shell gap.

The spectroscopic results for ^{36}Mg are gathered in Table I. The excitation energies are in good agreement with the present experimental result for the proposed 0^+ isomer and with the results of Ref. [17] for the yrast 2^+ and 4^+. Using the *EEdf1* interaction in the Monte Carlo shell model, we obtained a 0_2^+ energy of 2.32 MeV with a $B(E2)$ of 0.4 e^2 fm^4, using effective charges of 1.25 e and 0.25 e for protons and neutrons, respectively, which is not compatible with our observation. We must stress that the possible presence of a 0^+ isomer in ^{36}Mg is important beyond the value of its excitation energy.

TABLE I. Theoretical excitation energies (in MeV), Q_{spec} in e fm^2 and $B(E2)$'s (in e^2 fm^4), for ^{36}Mg, using the *sdpf-u-mix* interaction.

J^π	E (th)	Q_{spec}	J^π (f)	$B(E2)$
0_1^+	0.0			
2_1^+	0.58	-23	0_1^+	130
0_2^+	1.02		2_1^+	5
2_2^+	1.43	-15	0_1^+	2
2_2^+			2_1^+	1
2_2^+			0_2^+	120
4_1^+	1.73	-23	2_1^+	183
4_1^+			2_2^+	1

As mentioned above, our calculations with the *sdpf-u-mix* interaction show different nuclear structure depending on the energy of the 0_2^+ state, from a triaxial solution if it were not isomeric to a case of two coexisting prolate bands. Figure 4 and the $E2$ properties listed in Table I show the lowest band is dominated by $2\hbar\omega$ configurations and the excited one by $0\hbar\omega$ configurations. A very prominent feature of them is that the configuration mixing between the two bands is almost absent. In particular, the $B(E2)$ value from the isomer to the yrast 2^+ is small, compatible with the experimental value extracted from its lifetime. Let us mention finally that the crossover from the dominance of the $0f_{7/2}$ orbit to a massive occupation of the $1p_{3/2}$ orbit takes place at $N = 24$ as well, paving the way to the $N = 28$ island of inversion.

Conclusions. We observed a new 168-keV isomeric transition in ^{36}Mg, with a half-life of $90(^{+410}_{-50})_{\text{stat}}(\pm40)_{\text{tran}}(^{+800}_{-70})_{\text{sys}}$ ns with 3σ statistical and systematic uncertainties. From the observation of a 665-keV γ line in the prompt γ spectrum, we propose that it corresponds to a new 0^+ state at 833 keV deexciting to the known 665-keV 2^+ state [18]. To elucidate the microscopic origin of this isomer we performed shell-model calculations using the *sdpf-u-mix* interaction. We propose the observed low excitation energy of the state arises from two coexisting prolate-deformed configurations consisting of the normal-filling and intruder two-neutron excitations, respectively. We predict that, for $N > 20$ Mg isotopes, as the neutron $0f_{7/2}$ orbital is gradually filled, the $N = 20$ shell closure is restored while the $N = 28$ subshell closure is quenched. Therefore, the quasidegeneracy between normal and intruder configurations occurs only for ^{36}Mg. In contrast, other effective interactions used so far in the region predict substantial quenching of the $N = 20$ shell closure even past ^{38}Mg. We postulate the discrepancy arises from the inclusion, or lack of thereof, of three-body corrections into the monopole part of the effective interaction. The isomer presented in this work supports that ^{36}Mg is the bridge between the $N = 20$ island of inversion centered around ^{32}Mg and the $N = 28$ island of inversion centered in ^{40}Mg. As a direct consequence we anticipate no isomers will be present in ^{34,38}Mg. Thanks to the large yields of magnesium isotopes afforded at the recently commissioned FRIB facility in MSU (or RIKEN, Japan), this hypothesis may be tested in the near future.

[1] A. Poves and J. Retamosa, Phys. Lett. B **184**, 311 (1987).

[2] E. K. Warburton, J. A. Becker, and B. A. Brown, Phys. Rev. C **41**, 1147 (1990).

[3] K. Heyde and J. L. Wood, J. Phys. G: Nucl. Part. Phys. **17**, 135 (1991).

[4] N. Fukunishi, T. Otsuka, and T. Sebe, Phys. Lett. B **296**, 279 (1992).

[5] E. Caurier, F. Nowacki, and A. Poves, Phys. Rev. C **90**, 014302 (2014).

[6] C. Thibault, R. Klapisch, C. Rigaud, A. M. Poskanzer, R. Prieels, L. Lessard, and W. Reisdorf, Phys. Rev. C **12**, 644 (1975).

[7] G. Neyens, M. Kowalska, D. Yordanov, K. Blaum, P. Himpe, P. Lievens, S. Mallion, R. Neugart, N. Vermeulen, Y. Utsuno, and T. Otsuka, Phys. Rev. Lett. **94**, 022501 (2005).

[8] H. L. Crawford, P. Fallon, A. O. Macchiavelli, P. Doornenbal, N. Aoi, F. Browne, C. M. Campbell, S. Chen, R. M. Clark, M. L. Cortes, M. Cromaz, E. Ideguchi, M. D. Jones, R. Kanungo, M. MacCormick, S. Momiyama, I. Murray, M. Niikura, S. Paschalis *et al.*, Phys. Rev. Lett. **122**, 052501 (2019).

[9] T. Otsuka, T. Suzuki, R. Fujimoto, H. Grawe, and Y. Akaishi, Phys. Rev. Lett. **95**, 232502 (2005).

[10] Y. Utsuno, T. Otsuka, T. Mizusaki, and M. Honma, Phys. Rev. C **60**, 054315 (1999).

[11] N. Tsunoda, T. Otsuka, N. Shimizu, M. Hjorth-Jensen, K. Takayanagi, and T. Suzuki, Phys. Rev. C **95**, 021304(R) (2017).

[12] K. Fossez, J. Rotureau, N. Michel, and W. Nazarewicz, Phys. Rev. C **96**, 024308 (2017).

[13] J. H. Hamilton, A. V. Ramayya, W. T. Pinkston, R. M. Ronningen, G. Garcia-Bermudez, H. K. Carter, R. L. Robinson, H. J. Kim, and R. O. Sayer, Phys. Rev. Lett. **32**, 239 (1974).

[14] K. Wimmer, T. Kröll, R. Krücken, V. Bildstein, R. Gernhäuser, B. Bastin, N. Bree, J. Diriken, P. Van Duppen, M. Huyse, N. Patronis, P. Vermaelen, D. Voulot, J. Van de Walle, F. Wenander, L. M. Fraile, R. Chapman, B. Hadinia, R. Orlandi, J. F. Smith *et al.*, Phys. Rev. Lett. **105**, 252501 (2010).

[15] R. Elder, H. Iwasaki, J. Ash, D. Bazin, P. C. Bender, T. Braunroth, B. A. Brown, C. M. Campbell, H. L. Crawford, B. Elman, A. Gade, M. Grinder, N. Kobayashi, B. Longfellow, A. O. Macchiavelli, T. Mijatović, J. Pereira, A. Revel, D. Rhodes, J. A. Tostevin *et al.*, Phys. Rev. C **100**, 041301(R) (2019).

[16] A. Poves, J. Phys. G: Nucl. Part. Phys. **43**, 024010 (2016).

[17] P. Doornenbal, H. Scheit, S. Takeuchi, N. Aoi, K. Li, M. Matsushita, D. Steppenbeck, H. Wang, H. Baba, H. Crawford, C. R. Hoffman, R. Hughes, E. Ideguchi, N. Kobayashi, Y. Kondo, J. Lee, S. Michimasa, T. Motobayashi, H. Sakurai, M. Takechi *et al.*, Phys. Rev. Lett. **111**, 212502 (2013).

[18] P. Doornenbal, H. Scheit, S. Takeuchi, N. Aoi, K. Li, M. Matsushita, D. Steppenbeck, H. Wang, H. Baba, E. Ideguchi, N. Kobayashi, Y. Kondo, J. Lee, S. Michimasa, T. Motobayashi, A. Poves, H. Sakurai, M. Takechi, Y. Togano, and K. Yoneda, Phys. Rev. C **93**, 044306 (2016).

[19] H. L. Crawford, P. Fallon, A. O. Macchiavelli, R. M. Clark, B. A. Brown, J. A. Tostevin, D. Bazin, N. Aoi, P. Doornenbal, M. Matsushita, H. Scheit, D. Steppenbeck, S. Takeuchi, H. Baba, C. M. Campbell, M. Cromaz, E. Ideguchi, N. Kobayashi, Y. Kondo, G. Lee *et al.*, Phys. Rev. C **89**, 041303(R) (2014).

[20] F. Nowacki, A. Obertelli, and A. Poves, Prog. Part. Nucl. Phys. **120**, 103866 (2021).

[21] D. J. Morrissey, B. M. Sherrill, M. Steiner, A. Stolz, and I. Wiedenhoever, Nucl. Instrum. Methods Phys. Res., Sect. B **204**, 90 (2003).

[22] R. Yokoyama, M. Singh, R. Grzywacz, A. Keeler, T. T. King, J. Agramunt, N. T. Brewer, S. Go, J. Heideman, J. Liu, S. Nishimura, P. Parkhurst, V. H. Phong, M. M. Rajabali, B. C. Rasco, K. P. Rykaczewski, D. W. Stracener, J. L. Tain, A. Tolosa-Delgado, K. Vaigneur *et al.*, Nucl. Instrum. Methods Phys. Res., Sect. A **937**, 93 (2019).

[23] W. A. Peters, S. Ilyushkin, M. Madurga, C. Matei, S. V. Paulauskas, R. K. Grzywacz, D. W. Bardayan, C. R. Brune, J. Allen, J. M. Allen, Z. Bergstrom, J. Blackmon, N. T. Brewer, J. A. Cizewski, P. Copp, M. E. Howard, R. Ikeyama, R. L. Kozub, B. Manning, T. N. Massey *et al.*, Nucl. Instrum. Methods Phys. Res., Sect. A **836**, 122 (2016).

[24] C. J. Gross, T. N. Ginter, D. Shapira, W. T. Milner, J. W. Mcconnell, A. N. James, J. W. Johnson, J. Mas, P. F. Mantica, R. L. Auble, J. J. Das, J. L. Blankenship, J. H. Hamilton, R. L. Robinson, Y. A. Akovali, C. Baktash, J. C. Batchelder, C. R. Bingham, M. J. Brinkman, H. K. Carter *et al.*, Nucl. Instrum. Methods Phys. Res., Sect. A **450**, 12 (2000).

[25] M. Baginova, P. Vojtyla, and P. P. Povinec, Nucl. Instrum. Methods Phys. Res., Sect. A **897**, 22 (2018).

[26] A. Gade, P. Adrich, D. Bazin, M. D. Bowen, B. A. Brown, C. M. Campbell, J. M. Cook, S. Ettenauer, T. Glasmacher, K. W. Kemper, S. McDaniel, A. Obertelli, T. Otsuka, A. Ratkiewicz, K. Siwek, J. R. Terry, J. A. Tostevin, Y. Utsuno, and D. Weisshaar, Phys. Rev. Lett. **99**, 072502 (2007).

[27] N. Kobayashi, T. Nakamura, Y. Kondo, J. A. Tostevin, Y. Utsuno, N. Aoi, H. Baba, R. Barthelemy, M. A. Famiano, N. Fukuda, N. Inabe, M. Ishihara, R. Kanungo, S. Kim, T. Kubo, G. S. Lee, H. S. Lee, M. Matsushita, T. Motobayashi, T. Ohnishi *et al.*, Phys. Rev. Lett. **112**, 242501 (2014).

[28] S. Michimasa, Y. Yanagisawa, K. Inafuku, N. Aoi, Z. Elekes, Z. Fulop, Y. Ichikawa, N. Iwasa, K. Kurita, M. Kurokawa, T. Machida, T. Motobayashi, T. Nakamura, T. Nakabayashi, M. Notani, H. J. Ong, T. K. Onishi, H. Otsu, H. Sakurai, M. Shinohara *et al.*, Phys. Rev. C **89**, 054307 (2014).

[29] N. Tsunoda, T. Otsuka, K. Takayanagi, N. Shimizu, T. Suzuki, Y. Utsuno, S. Yoshida, and H. Ueno, Nature (London) **587**, 66 (2020).

[30] E. Caurier, G. Martínez-Pinedo, F. Nowacki, A. Poves, and A. P. Zuker, Rev. Mod. Phys. **77**, 427 (2005).

[31] N. Shimizu, T. Mizusaki, Y. Utsuno, and Y. Tsunoda, Comput. Phys. Commun. **244**, 372 (2019).